POLDER observations of cloud bidirectional reflectances compared to a plane-parallel model using the International Satellite Cloud Climatology Project cloud phase functions

Jacques Descloitres, Jean-Claude Buriez, Frédéric Parol, Y. Fouquart

JOURNAL OF GEOPHYSICAL RESEARCH, VOL. 103, NO. D10, PAGES 11,411–11,418, MAY 27, 1998

POLDER observations of cloud bidirectional reflectances compared to a plane-parallel model using the International Satellite Cloud Climatology Project cloud phase functions

J. Descloitres,[1] J. C. Buriez, F. Parol, and Y. Fouquart

Laboratoire d'Optique Atmosphérique, Université des Sciences et Technologies de Lille, Villeneuve d'Ascq, France

Abstract. This study investigates the validity of the plane-parallel cloud model and in addition the suitability of water droplet and ice polycrystal phase functions for stratocumulus and cirrus clouds, respectively. To do that, we take advantage of the multidirectional viewing capability of the Polarization and Directionality of the Earth's Reflectances (POLDER) instrument which allows us to characterize the anisotropy of the reflected radiation field. We focus on the analysis of airborne-POLDER data acquired over stratocumulus and cirrus clouds during two selected flights (on April 17 and April 18, 1994) of the European Cloud and Radiation Experiment (EUCREX'94) campaign. The bidirectional reflectances measured in the 0.86 μm channel are compared to plane-parallel cloud simulations computed with the microphysical models used by the International Satellite Cloud Climatology Project (ISCCP). Although clouds are not homogeneous plane-parallel layers, the extended cloud layers under study appear to act, on average, as a homogeneous plane-parallel layer. The standard water droplet model (with an effective radius of 10 μm) used in the ISCCP analysis seems to be suitable for stratocumulus clouds. The relative root-mean-square difference between the observed bidirectional reflectances and the model is only 2%. For cirrus clouds, the water droplet cloud model is definitely inadequate since the rms difference rises to 9%; when the ice polycrystal model chosen for the reanalysis of ISCCP data is used instead, the rms difference is reduced to 3%.

1. Introduction

Because of their multiple interactions with radiation in the Earth's surface-atmosphere system, clouds play an important role in the Earth radiation budget and consequently have a strong impact on the climate. In order to improve the estimate of their influence on the evolution of the climate, recent general circulation models predict the cloud condensed water content and then derive radiative properties of clouds [e.g., *Cess et al.*, 1996]. However, a small variation in cloud characteristics could have a large influence on the evolution of the climate [*Senior and Mitchell*, 1993]. Consequently, there is a clear need of long-term observations of the Earth radiation balance and cloud properties. In this way, the International Satellite Cloud Climatology Project (ISCCP) has been designed to establish a climatology of cloud properties at the global scale [*Rossow and Schiffer*, 1991].

One of the most significant cloud parameters used to determine the cloud-radiation interactions is the cloud optical thickness, which is directly related to the cloud particle size distribution and the condensed water path. Programs like ISCCP try to retrieve the cloud optical thickness from satellite measurements of visible radiances. In practice, all radiometers so far are based on the same principle of a single detector plus a scanning mechanism which allows us to observe a target from only one single direction per overpass. However, the radiation outgoing from any target depends on the angle of observation. To compensate for the lack of observation of this angular dependence, one has to provide additional information. In ISCCP, this is done by assuming that the clouds are plane-parallel layers with a prescribed cloud particle size distribution; under these conditions, the radiative transfer theory predicts the angular dependence of the reflected radiation. If the model is wrong, the relationship between the radiance observed in the satellite direction and the optical thickness is inadequate and the retrieval fails. The magnitude of the corresponding error depends on the cloud type as well as on the conditions of observation and illumination.

The angular dependence of the reflected solar radiation can be characterized by the cloud bidirectional reflectance

$$\rho_\nu(\mu_0,\mu,\varphi) = \frac{\pi L_\nu(\mu_0,\mu,\varphi)}{\mu_0 E_{0\nu}}, \qquad (1)$$

where μ_0 is the cosine of the solar zenith angle, μ is the cosine of the viewing zenith angle, φ is the relative azimuth angle measured with respect to the solar plane, $L_\nu(\mu_0,\mu,\varphi)$ is the upward radiance at wavenumber ν in the viewing direction (μ,φ), and $\mu_0 E_{0\nu}$ is the incident solar flux.

Only few direct observations of cloud bidirectional reflectance have been compared to radiation fields calculated using the plane-parallel cloud model. *Davis and Cox* [1982] constructed empirical cloud models from airborne multidetector

[1]Now at Department of Geography, University of Maryland, College Park.

Paper number 98JD00592.
0148-0227/98/98JD-00592$09.00

measurements. They compared their altostratus cloud model to plane-parallel simulations. They obtained a rather good agreement in the solar plane except in the backward direction. *Stuhlmann et al.* [1985] also constructed empirical cloud models but from Nimbus 7 Earth Radiation Budget (ERB) and Geostationary Operational Environmental Satellite (GOES) data. Their comparison between theoretical and empirical models showed a rather good agreement, about 10% for solar zenith angles lower than 70°. *Descloitres et al.* [1995] used the Polarization and Directionality of the Earth's Reflectances (POLDER) airborne simulator during the Atlantic Stratocumulus Transition Experiment (ASTEX). They found that the bidirectional reflectances of a solid stratocumulus cloud deck compare favorably (within 2-3%) with those of plane-parallel layers composed of liquid water drops. *Spinhirne et al.* [1996] used the Tilt Scan CCD Camera (TSCC) radiometer during the First ISCCP Regional Experiment (FIRE II) to measure the bidirectional reflectance of cirrus clouds in the solar plane. They compared their observations to plane-parallel cloud model calculations based on various cloud phase function models. The measured angular reflectance pattern was flatter than predicted by the models. The agreement of measurements with the liquid water model was very poor. A better agreement was obtained for a phase function derived by *Takano and Liou* [1989] for cirrostratus ice crystal columns, but in some cases a simple Henyey-Greenstein phase function gave better comparison, although the authors did not conclude that this phase function was generally appropriate or superior to the ice column model. The aim of this study is to contribute to such comparisons, using POLDER airborne simulator data acquired over extended stratocumulus and cirrus clouds during the European Cloud and Radiation Experiment (EUCREX'94) [*Raschke et al.*, 1998], which is the continuation of the International Cirrus Experiment (ICE) [*Raschke et al.*, 1990]. Indeed, the multidirectional viewing capability of the POLDER instrument allows us to observe a part of the bidirectional reflectance distribution function (BRDF) of any scene. It is thus possible to investigate the validity of the plane-parallel cloud model and in addition the suitability of water droplet and ice polycrystal phase functions for stratocumulus and cirrus clouds, respectively. More particularly, the two phase functions routinely used in the ISCCP scheme [*Rossow et al.*, 1996] will be considered.

The POLDER data used in this study are described in section 2. A method for constructing BRDFs representative of the observed cloud types is presented in section 3. Then, in section 4, observations are compared to simulations based on the cloud microphysics used in the ISCCP scheme. Conclusions are given in section 5.

2. Data

POLDER is an instrument designed and built by the Laboratoire d'Optique Atmosphérique (LOA) and the Centre National d'Etudes Spatiales, France (CNES). It is devoted to the global observation of polarization and directionality of the solar radiation reflected by the Earth's surface-atmosphere system. The instrument was launched in August 1996 aboard the Japanese Advanced Earth Observing Satellite (ADEOS) platform. One of the scientific objectives of the satellite mission concerns the cloud characteristics: BRDF, optical thickness, pressure, and phase. Here we limit our study to the cloud bidirectional reflectance measured in the 0.86 μm channel of the airborne POLDER simulator and the cloud optical thickness retrieved from those measurements.

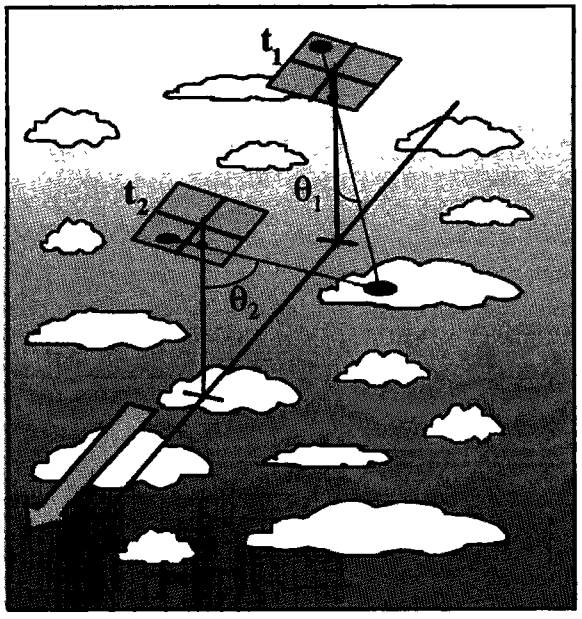

Figure 1. Schematic representation of the observational mode of POLDER. As the aircraft moves between successive acquisitions of POLDER, a given target appears on several locations on the charge-coupled device array detector under different viewing angles. Two observations (at time t_1 and t_2) of a target are represented; θ_1 and θ_2 are the corresponding viewing zenith angles.

During the EUCREX campaign in April 1994, POLDER was flown over stratocumulus and cirrus clouds aboard the German Falcon of the Deutsche Forschungsanstalt für Luft und Raumfahrt (DLR). The western part of Brittany, over the Atlantic Ocean, had been chosen for the aircraft missions. This paper focuses on two flights performed on the afternoon of April 17, 1994, and on the morning of April 18, 1994, corresponding to visually extended thick cirrus and stratocumulus cloud layers, respectively.

On April 17, the meteorological analysis indicated a high-pressure system located over the North Atlantic Ocean, Ireland, and England. A low was centered on southern France, spreading from Spain to northern Italy. One day before (April 16), this low was located northeast of Europe. It was connected to another cyclonic depression centered north of Iceland and Sweden, making the jet stream stronger and leading cold polar air over northern Europe. That resulted in the formation of a wide cirrus cloud deck throughout the experimental area on April 17. The cloud top was located between 9 km and 10 km, say, at a temperature of 220 K. The cloud base was around 6 km at a temperature of about 250 K. Microphysical measurements lead to an effective radius of equivalent spherical particles around 24 μm [*Sauvage et al.*, 1998]. The hereafter reported data have been acquired at flight altitude of 10,700 m.

On April 18, air from the northeast entered the experimental area between a ridge of high pressure centered east of Ireland and a low located over central Europe; this resulted in wide stratocumulus fields throughout the English Channel, over western France, and in the Bay of Biscay. The cloud depth was only 200 m, but the stratocumulus was optically thick. The cloud top height was varying from 800 m to 1100 m. The aircraft flight altitude was 3050 m.

The POLDER instrument is composed of a charge-coupled device (CCD) array detector, a rotating wheel which carries spectral and polarizing filters, and a wide field of view lens (see *Deschamps et al.* [1994] for further details). The instrument field of view of the airborne simulator extends up to ± 52° in the along-track direction and ± 42° in the cross-track direction. Angular deviations due to the pitch and roll of the aircraft are taken into account. The CCD array is composed of 288 x 242 pixels. Considering the typical aircraft-cloud relative altitude, it corresponds to a scene of 9 km x 7 km for low-level clouds and 2.2 km x 1.8 km for high-level clouds; the respective spatial resolution of the instrument is 25 m and 8 m. However, the resolution is degraded to 10 x 10 pixels in order to reduce both the data flow and the measurement noise. Therefore the typical size of a cloud target is 250 m for low-level clouds and 80 m for high-level clouds. The aircraft displacement between two successive acquisitions of POLDER is around 1 km.

An original feature of POLDER is its ability to provide multidirectional reflectance measurements of any scene. As illustrated in Figure 1, a given target is seen under several viewing directions. The number of directions depends on the aircraft speed and the aircraft-cloud relative altitude. Typically, it was 9 directions for low-level clouds and 2 for high-level clouds during EUCREX'94. Figure 2 presents an example of POLDER images acquired over a stratocumulus cloud deck. The same geographical target appears several times on this set of images but at different locations on the CCD array; that means this target is observed under different viewing angles. For instance, in Figure 2, the same hole is clearly seen on the images number 85 and 90 (dark part of the images). However, directional effects like the backscatter spot appear at the same location (at bottom right) on all images.

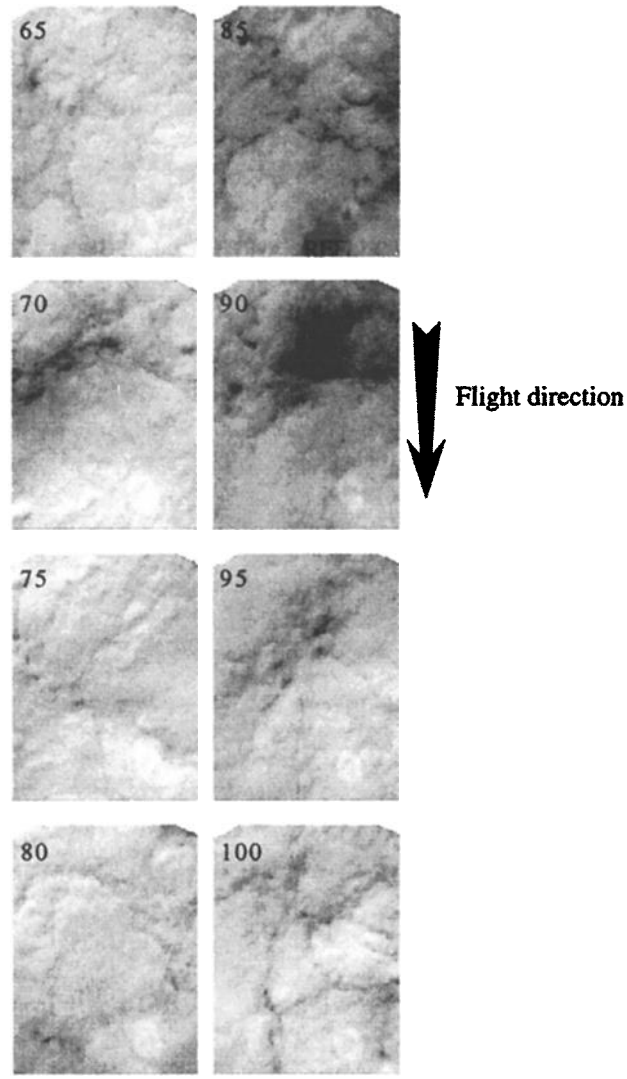

Figure 2. Example of POLDER images acquired during the European Cloud and Radiation Experiment (EUCREX'94) (mission 206, April 18, 1994, images 65-100) over a stratocumulus cloud deck off the coast of Brittany, France. Every fifth image of the sequence is reported. The gray shading corresponds to reflectance values varying from 0 to 1.0.

3. Methodology

In order to analyze the anisotropy of the radiation reflected by the observed clouds, a first possible approach is based on the fact that any geographical target is observed under several (typically 9 for low-level clouds) viewing angles. The POLDER pixels can be related to geographical coordinates at the cloud level, and then a given target can be located on successive images. For each target, the set of measured values of bidirectional reflectance can be compared to the plane-parallel model at the corresponding viewing angles.

Another approach consists in analyzing the bidirectional reflectance over the whole field of view of POLDER. Indeed, if a cloudy scene observed by POLDER were perfectly homogeneous, a single image could be considered as a cloud BRDF pattern limited to the solid angle Ω corresponding to the instrument field of view. In fact, each detector of the CCD array sees a different part of the cloud. It results that variations in bidirectional reflectance are due both to the anisotropy of the radiation reflected by the scene and to the horizontal variations in optical thickness from one cloud target to another within the instrument field of view. In order to remove the last effect and to characterize the anisotropy itself, the simplest approach consists in averaging a sequence of successive images. The BRDF pattern of the average image is then considered as the BRDF pattern of one equivalent target representative of the scene.

Descloitres et al. [1995] applied both approaches to POLDER data acquired during ASTEX above a stratocumulus cloud deck. Not surprisingly, the results obtained from averaged images and from the target-by-target method were quite similar; in both cases, the rms difference between the observed and the modeled reflectances was about 2-3%. Indeed, averaging whole images along a flight leg is equivalent to constructing one BRDF pattern from the measured bidirectional reflectances of all the targets of the leg.

The target-by-target method presents some limitations. When the cloud top height varies a lot along a flight leg, the altitude of a target becomes uncertain, and thus it is difficult to locate targets on successive images. Moreover, the number of viewing angles for each target decreases drastically as the cloud top height draws near to the aircraft level; it is reduced to 2 directions for high-level clouds observed from the Falcon. Therefore we chose the simple average method, in order to present both a stratocumulus case and a cirrus case with the same method.

For the average BRDF calculation, we define the average bidirectional reflectance of a series of images as

$$\langle\rho\rangle_N(\mu_0,\mu,\varphi) = \frac{1}{N}\sum_{i=1}^{N}\rho_i(\mu_0,\mu,\varphi), \quad (2)$$

where N is the number of averaged images and $\rho_i(\mu_0,\mu,\varphi)$ is the bidirectional reflectance value of the image i. We also define the average pseudoalbedo $\tilde{\alpha}_N(\mu_0)$ of the series of images,

$$\tilde{\alpha}_N(\mu_0) = \frac{\iint_\Omega \langle\rho\rangle_N(\mu_0,\mu,\varphi)\,\mu\,d\mu\,d\varphi}{\iint_\Omega \mu\,d\mu\,d\varphi}, \quad (3)$$

where the integration is over the solid angle Ω limited by the instrument field of view.

The average BRDF pattern obtained with (2) can actually be considered as representative of one scene if each detector of the CCD array sees a similar distribution of targets. In other words, the scene can be very inhomogeneous, but each pixel must see the same variability. In a first step, when averaging successive images, we assume their number N becomes sufficiently large when the averaged BRDF becomes stationary, that is, the difference between $\langle\rho\rangle_{N-1}$ and $\langle\rho\rangle_N$ tends toward zero. Therefore we define a variability rate as

$$\zeta(N,N-1) = \frac{1}{\tilde{\alpha}_N(\mu_0)} \times \left(\frac{\iint_\Omega \left[\langle\rho\rangle_N(\mu_0,\mu,\varphi) - \langle\rho\rangle_{N-1}(\mu_0,\mu,\varphi)\right]^2 \mu\,d\mu\,d\varphi}{\iint_\Omega \mu\,d\mu\,d\varphi}\right)^{\frac{1}{2}}. \quad (4)$$

The variability rate decreases more or less quickly as N increases, according to the repetitivity of cloud inhomogeneities along the flight leg. From the inspection of various observations, a threshold of 0.5% was chosen for $\zeta(N,N-1)$. This threshold is reached after averaging a few tens of images typically (see Figure 3). However, the analysis of many POLDER observations shows that this criterion is sometimes insufficient to obtain a BRDF pattern representative of one scene. Indeed, the average BRDF can remain asymmetric in relation to the principal plane when a singular target with an exceedingly high or low reflectance is seen under a limited range of viewing directions. In that case, the distribution of observed targets differs from one viewing angle to another over the whole field of view. Thus we define an azimuthal asymmetry rate by

$$\xi(N) = \frac{1}{2\,\tilde{\alpha}_N(\mu_0)} \times \left(\frac{\iint_\Omega \left[\langle\rho\rangle_N(\mu_0,\mu,\varphi) - \langle\rho\rangle_N(\mu_0,\mu,-\varphi)\right]^2 \mu\,d\mu\,d\varphi}{\iint_\Omega \mu\,d\mu\,d\varphi}\right)^{\frac{1}{2}}, \quad (5)$$

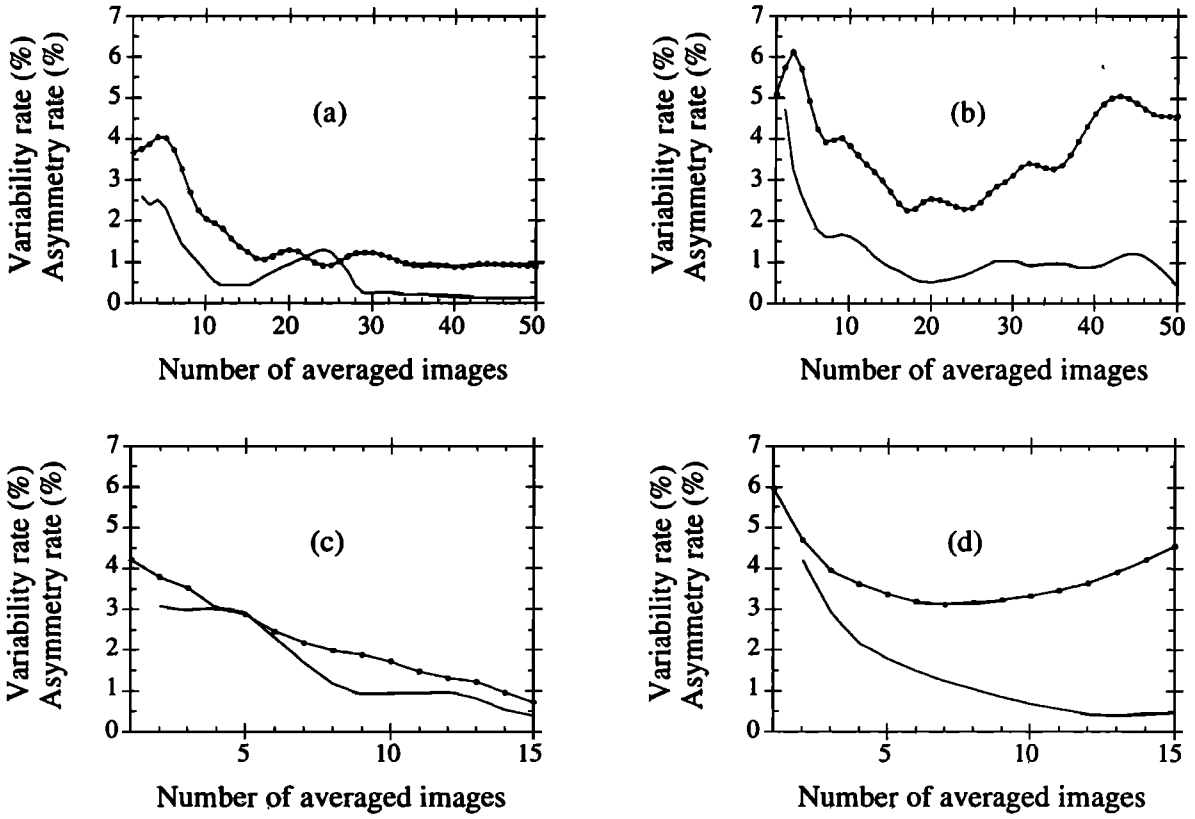

Figure 3. Variability (solid curve) and asymmetry (dotted curve) rates as a function of the number of averaged images for different cloud types observed from POLDER. Sequences corresponding to a stratocumulus cloud (EUCREX, mission 206, April 18, 1994) are shown: (a) images 65-114 and (b) images 116-165. Also sequences corresponding to a cirrus cloud (EUCREX, mission 205, April 17, 1994) are shown: (c) images 723-737 and (d) images 689-703.

which tends toward zero when the mean BRDF becomes symmetric in relation to the principal plane. For two scenes with similar variability rates, different asymmetry rates can be observed (compare Figures 3a to 3b and Figures 3c to 3d).

Practically, N is chosen such as $\zeta(N,N-1)$ is lower than 0.5% and $\xi(N)$ is lower than 1% (sequences shown in Figures 3a and 3c can be retained, whereas sequences in Figures 3b and 3d are rejected). Under these conditions, the anisotropy of the radiation reflected by an inhomogeneous scene is well characterized since the noise related to differences between the distribution of observed targets from one viewing direction to another is expected to be reduced to about 1%. Note that, because of the asymmetry rate criterion, scenes where the structure of cloud inhomogeneities depends on a particular direction (e.g., cloud streets) are excluded from this study.

4. Results

The cloud BRDF patterns measured from POLDER have been compared to computations of bidirectional reflectance based on the plane-parallel approximation. These calculations have been performed by using the discrete ordinate method [*Stamnes et al.*, 1988]. The ocean surface is modeled following *Cox and Munk* [1956]. The effect of standard aerosols [*World Climate Programme*, 1986] and molecules is taken into account. The clouds are assumed to be homogeneous plane-parallel layers composed of the same particles as in the new ISCCP cloud analysis procedure [*Rossow et al.*, 1996]. The microphysical model for liquid water clouds is a gamma distribution of spherical liquid water drops with an effective radius of 10 μm and an effective variance of 0.15 [*Hansen and Travis*, 1974]. In the first ISCCP analysis [*Rossow and Schiffer*, 1991], that model was used for all cloud types. Now, an ice crystal model with a random fractal crystal shape [*Macke*, 1996] is used for high-level clouds; it corresponds to a −2 power law size distribution with an effective radius of 30 μm and an effective variance of 0.10 [*Mishchenko et al.*, 1996]. The respective phase function of the two microphysical models is plotted in Figure 4.

For a sequence of POLDER images, the mean observed reflectance $\langle\rho\rangle_N(\mu_0,\mu,\varphi)$ over N images can be compared to the

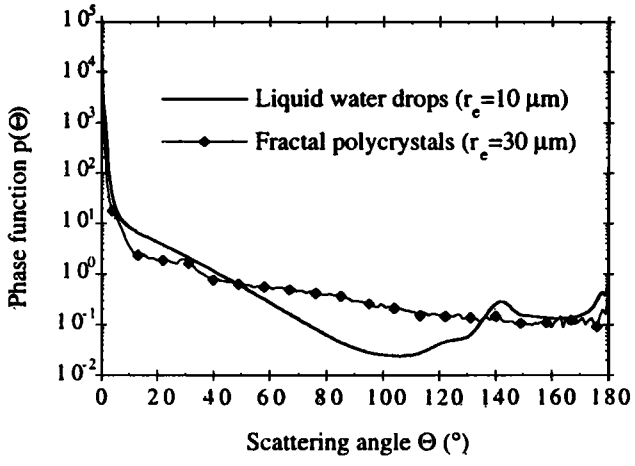

Figure 4. Phase function for a size distribution of liquid water drops (effective radius r_e is 10 μm) and a size distribution of fractal polycrystals (effective radius r_e is 30 μm).

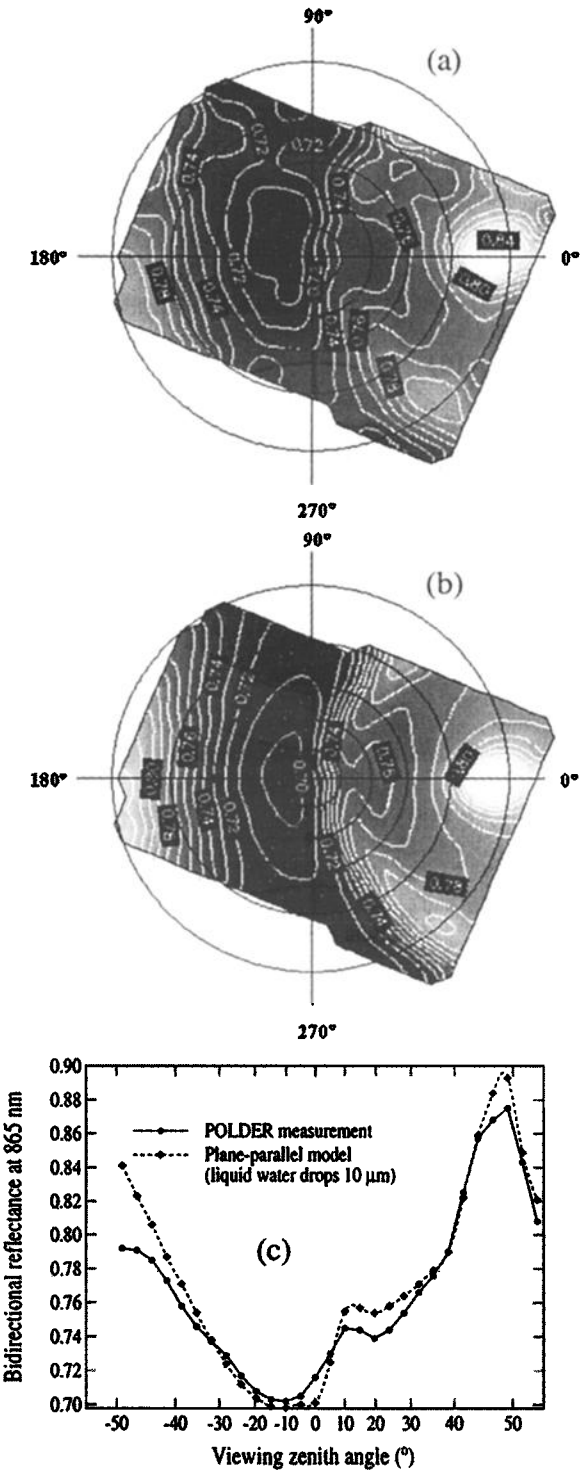

Figure 5. Comparison between (a) the bidirectional reflectance distribution function (BRDF) at 0.86 μm of a stratocumulus cloud observed by POLDER (EUCREX, mission 206, April 18, 1994, images 65-100) and (b) the one of the nearest plane-parallel layer, computed using the International Satellite Cloud Climatology Project (ISCCP) model (spherical drops with r_e equal to 10 μm). The rms difference is σ_{PP} = 1.9%. The concentric circles correspond to viewing zenith angles 10°, 20°, ..., 50° (from inside to outside). Azimuth 0° corresponds to the backscatter direction. (c) The cross section in the principal plane. The positive viewing zenith angles are toward the Sun, and the negative angles are toward the antisolar location. The solar zenith angle is equal to 47°.

modeled reflectance $\rho_{PP}(\mu_0,\mu,\varphi)$ of the nearest plane-parallel model, of which the cloud optical thickness is adjusted so that the plane-parallel pseudoalbedo defined by (3) is equal to the observed one, that is,

$$\tilde{\alpha}_{PP}(\mu_0) = \tilde{\alpha}_N(\mu_0). \quad (6)$$

The discrepancy between the POLDER measurements and the plane-parallel model is characterized by the relative weighted root-mean-square difference $\sigma_{PP}(N)$ defined as

$$\sigma_{PP}(N) = \frac{1}{\tilde{\alpha}_N(\mu_0)} \times \left(\frac{\iint_\Omega \left[\langle\rho\rangle_N(\mu_0,\mu,\varphi) - \rho_{PP}(\mu_0,\mu,\varphi)\right]^2 \mu \, d\mu \, d\varphi}{\iint_\Omega \mu \, d\mu \, d\varphi} \right)^{\frac{1}{2}}. \quad (7)$$

When considering low-level clouds, some previous results have already shown that the model for liquid water clouds is roughly suitable for stratocumulus clouds observed by POLDER [*Descloitres et al.*, 1995]. Because of horizontal inhomogeneities, they are not homogeneous plane-parallel layers over one single POLDER image, with $\sigma_{PP}(N=1) \sim 10\%$, but they act on average as a homogeneous plane-parallel layer for a sequence of images, with $\sigma_{PP}(N\sim50) \sim 2\%$. As illustrated in Figure 5, the results obtained from POLDER measurements of the EUCREX campaign are quite similar to those of the ASTEX campaign, as presented by *Descloitres et al.* [1995]. Particularly, the backscatter peak and the cloudbow are clearly visible on the mean observed BRDF pattern, whereas they are hardly distinguishable on single images (see Figure 2).

With regard to cirrus clouds, scattering by ice crystals is known to be very different from spheres and very sensitive to crystal shapes [e.g., *Takano and Liou*, 1989]. Therefore, as shown in Figure 6, the use of one microphysical model for all clouds in an interpretation of satellite data, as in the first ISCCP algorithm, is a source of strong uncertainties for the retrieved characteristics of ice crystal clouds. For that reason, the fractal polycrystals of *Macke* [1996], which are expected to be representative of irregularly shaped and randomly oriented ice particles, were introduced into the new ISCCP algorithm to model scattering properties of cirrus clouds. As illustrated in Figure 6, a good agreement between that model and the first observations of POLDER over cirrus clouds is observed ($\sigma_{PP}(N\sim15) \sim 3\%$), whereas the model for liquid water clouds is definitely inadequate ($\sigma_{PP}(N\sim15) \sim 9\%$). In particular, the relative difference between modeled and observed reflectances in the backscatter direction is 4% with the polycrystal model, but it reaches 20% with the droplet model.

When we have one single viewing direction, the optical thickness must be retrieved from that single radiance measurement, as in ISCCP, for example; clearly some error can be expected from the dependence of the retrieval on the available viewing direction. To illustrate the additional information given by the multidirectional capability of POLDER, Figure 6 also compares the cloud optical thickness retrieved from one single direction to the one obtained when using all available viewing directions. The dependence of the retrieved optical thickness on the viewing angle is notably reduced with the ice polycrystal model as compared to the water droplet model.

5. Conclusion

The airborne measurements of POLDER clearly illustrate the importance of multidirectional observations to estimate errors when cloud properties are retrieved by using the plane-parallel assumption. Although clouds are not homogeneous plane-parallel layers, the extended cloud layers observed by the airborne version of POLDER during the EUCREX campaign appear to act on average as a homogeneous plane-parallel layer.

As given by *Descloitres et al.* [1995], the standard water droplet model (with an effective radius of 10 μm) used in the ISCCP analysis seems to be suitable for stratocumulus clouds. The relative root-mean-square difference between the observed bidirectional reflectances and the model is only 2%. This rms difference is hardly reduced when the effective radius is changed to obtain a better fit.

With regard to ice crystal clouds, the POLDER observations underline the need of a phase discrimination in the analysis of satellite data. Furthermore, we found an encouraging agreement between our first measurements over cirrus clouds and the polycrystal model used in the new ISCCP algorithm. For ice crystal clouds, the water droplet model is definitely inadequate since the relative root-mean-square difference between modeled and observed bidirectional reflectances rises to 9%. When the polycrystal model is used instead, the difference is reduced to 3%. However, we cannot conclude that the polycrystal model is generally appropriate for all the cirrus clouds.

The suitability of the plane-parallel cloud model does not imply that the retrieved cloud optical thickness is accurate. *Cahalan et al.* [1994] have considered a fractal cloud model which simulates the horizontal variability observed in marine stratocumulus clouds. They found that the cloud albedo is approximated properly by a plane-parallel model having an optical thickness typically 30% smaller than the actual mean optical thickness. Therefore the cloud optical thickness derived from a plane-parallel model has to be considered as an "effective" optical thickness. The suitability of the plane-parallel model to our measurements over stratocumulus clouds suggests that the net horizontal photon transport can be ignored at the observed scale (250 m). In other words, the independent pixel approximation is valid for that resolution, since the mean reflectance of a distribution of cloud targets is very close to the plane-parallel model. Thus the break in the scaling properties of stratocumulus cloud scenes, which appears generally around 200-400 m [*Davis et al.*, 1997], would be below 250 m in the present case study.

Our analysis was restricted to extended thick clouds. Features similar to those here reported were obtained from the other flights made over extended thick stratocumulus clouds during ASTEX and EUCREX experiments. However, the cirrus case analyzed in this paper is a rare case of extended thick high-level cloud observed by the POLDER airborne simulator. Therefore the conclusions about the plane-parallel model concern neither the broken stratocumulus clouds nor the whole of high-level clouds. The spaceborne version of POLDER should allow us to perform similar comparisons between observed and modeled bidirectional reflectances at extended scale, using a target-by-target method. Operational algorithms have been developed in this way [*Buriez et al.*, 1997]. So we hope it will be possible to quantify the validity of the plane-parallel approximation at the global scale.

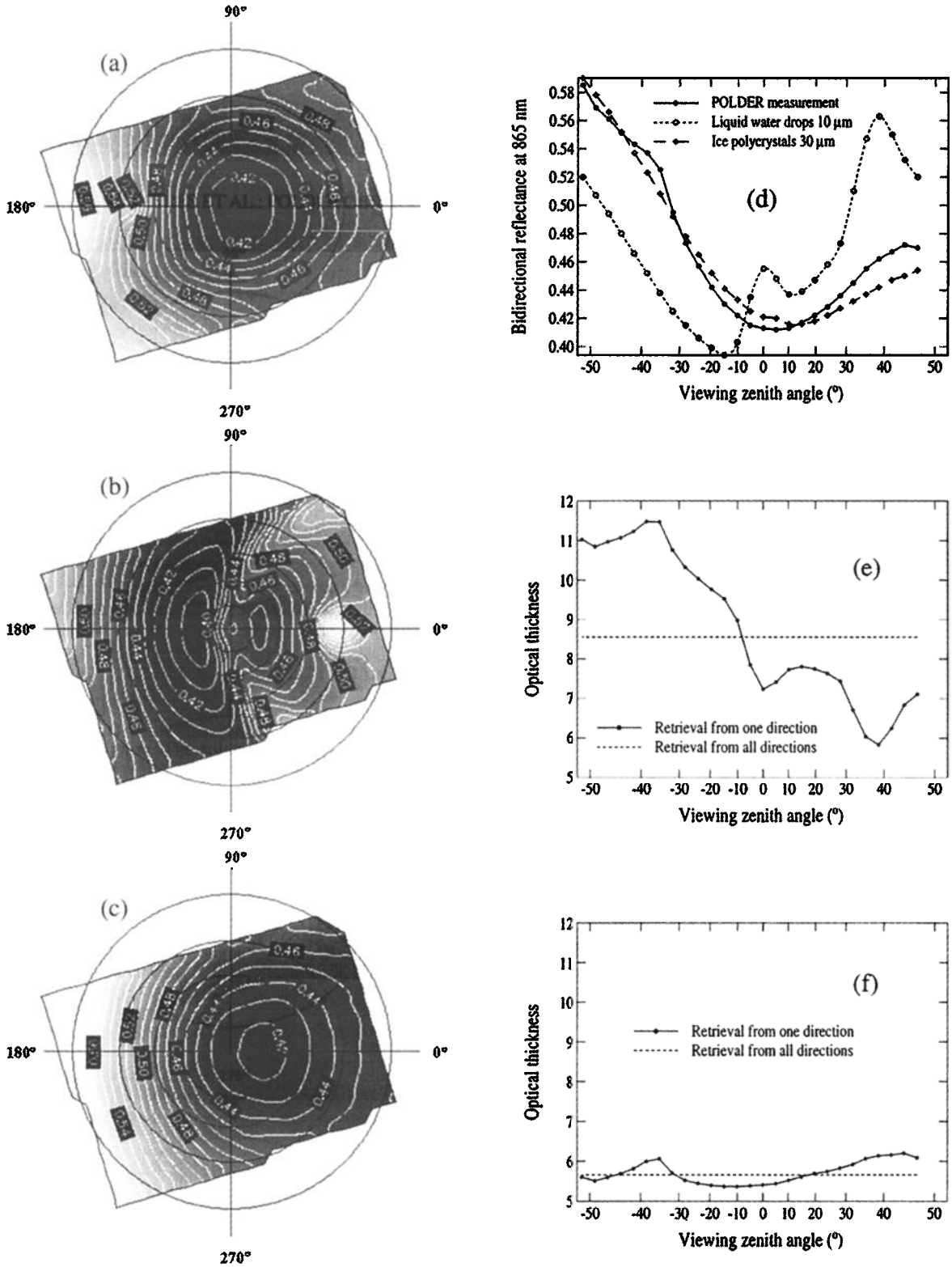

Figure 6. Comparison between (a) the bidirectional reflectance distribution function (BRDF) at 0.86 µm of a cirrus cloud observed by POLDER (EUCREX, mission 205, April 17, 1994, images 725-737) and the one of the nearest plane-parallel layer, computed using the ISCCP model for (b) liquid water clouds and (c) ice crystal clouds (fractal polycrystals with r_e equal to 30 µm). The rms difference σ_{PP} is 8.3% for liquid water clouds and 2.8% for ice crystal clouds. (d) The cross section in the principal plane. The optical thickness which would be retrieved using one single radiance measurement, compared to the one retrieved using the whole field of view, is shown, corresponding (e) to the water droplet phase function and (f) to the ice crystal phase function. The positive viewing zenith angles are toward the Sun, and the negative angles are toward the antisolar location. The solar zenith angle is equal to 38°.

Acknowledgments. This work was supported by the European Economic Community (EEC) and the Centre National d'Etudes Spatiales (CNES). The authors are grateful to F. Lemire for his help in processing the POLDER data. They thank A. Macke and M. Mishchenko for providing useful information about the polycrystal phase function. Pr. E. Raschke is acknowledged for his leading activity in EUCREX.

References

Buriez, J. C., C. Vanbauce, F. Parol, P. Goloub, M. Herman, B. Bonnel, Y. Fouquart, P. Couvert, and G. Seze, Cloud detection and derivation of cloud properties from POLDER, *Int. J. Remote Sens., 18*, 2785-2813, 1997.

Cahalan, R. F., W. Ridgway, W. J. Wiscombe, S. Gollmer, and Harshvardhan, Independent pixel and Monte Carlo estimates of stratocumulus albedo, *J. Atmos. Sci., 51*, 3776-3790, 1994.

Cess, R. D., et al., Cloud feedback in atmospheric general circulation models: An update, *J. Geophys. Res., 101*, 12,791-12,794, 1996.

Cox, C., and W. Munk, Slopes of the sea surface deduced from photographs of Sun glitter, *Bull. Scripps Int. Oceanogr., 6*, 401-488, 1956.

Davis, J. M., and S. K. Cox, Reflected solar radiances from regional scale scenes, *J. Appl. Meteorol., 21*, 1698-1712, 1982.

Davis, A., A. Marshak, R. Cahalan, and W. Wiscombe, The Landsat scale break in stratocumulus as a three-dimensional radiative transfer effect: Implications for cloud remote sensing, *J. Atmos. Sci., 54*, 241-260, 1997.

Deschamps, P. Y., F. M. Bréon, M. Leroy, A. Podaire, A. Bricaud, J. C. Buriez, and G. Sèze, The POLDER mission: Instrument characteristics and scientific objectives, *IEEE Trans. Geosci. Remote Sens., 32*, 598-615, 1994.

Descloitres, J., F. Parol, and J. C. Buriez, On the validity of the plane-parallel approximation for cloud reflectances as measured from POLDER during ASTEX, *Ann. Geophys., 13*, 108-110, 1995.

Hansen, J. E., and L. D. Travis, Light scattering in planetary atmospheres, *Space Sci. Rev., 16*, 527-610, 1974.

Macke, A., Single scattering properties of atmospheric ice crystals, *J. Atmos. Sci., 53*, 2813-2825, 1996.

Mishchenko, M. I., W. B. Rossow, A. Macke, and A. A. Lacis, Sensitivity of cirrus cloud albedo, bidirectional reflectance and optical thickness retrieval accuracy to ice particle shape, *J. Geophys. Res., 101*, 16,973-16,985, 1996.

Raschke, E., J. Schmetz, J. Heintzenberg, R. Kandel, and R. Saunders, The International Cirrus Experiment (ICE) - A joint European effort, *Eur. Space Agency J., 14*, 193-199, 1990.

Raschke, E., P. Flamant, Y. Fouquart, P. Hignett, H. Isaka, P. Jonas, and H. Sundqvist, Cloud-radiation studies during the European Cloud and Radiation Experiment (EUCREX), *Surv. Geophys.*, in press, 1998.

Rossow, W. B., and R. A. Schiffer, ISCCP cloud data products, *Bull. Am. Meteorol. Soc., 72*, 2-20, 1991.

Rossow, W. B., A. W. Walker, D. E. Beuschel, and M. D. Roiter, International Satellite Cloud Climatology Project (ISCCP): Documentation of new cloud data sets, *WMO/TD 737*, 115 pp., World Meteorol. Organ., Geneva, 1996.

Sauvage, L., H. Chepfer, V. Trouillet, P. H. Flamant, G. Brogniez, J. Pelon, and F. Albers, Remote sensing of Cirrus radiative parameters during EUCREX'94: Case study of 17 April 1994, 1, Observations, *Mon. Weather. Rev.*, in press, 1998.

Senior, C. A., and J. F. B. Mitchell, Carbon dioxide and climate: The impact of cloud parameterization, *J. Clim., 6*, 393-418, 1993.

Spinhirne, J. D., W. D. Hart, and D. L. Hlavka, Cirrus infrared parameters and shortwave reflectance relations from observations, *J. Atmos. Sci., 53*, 1438-1458, 1996.

Stamnes, K., S. C. Tsay, W. Wiscombe, and K. Jayaweera, Numerically stable algorithm for discrete-ordinate method radiative transfer in multiple scattering and emitting layered media, *Appl. Opt., 27*, 2502-2509, 1988.

Stuhlmann, R., P. Minnis, and G. L. Smith, Cloud bidirectional reflectance functions: A comparison of experimental and theoretical results, *Appl. Opt., 24*, 396-401, 1985.

Takano, Y., and K. N. Liou, Solar radiative transfer in cirrus clouds, I, Single scattering and optical properties of hexagonal ice crystals, *J. Atmos. Sci., 46*, 3-19, 1989.

World Climate Programme, A preliminary cloudless standard atmosphere for radiation computation, *Rep. WCP-112*, 53 pp., Radiat. Comm., Boulder, Colo., 1986.

J. C. Buriez, Y. Fouquart, and F. Parol, Laboratoire d'Optique Atmosphérique, Université des Sciences et Technologies de Lille, 59655 Villeneuve d'Ascq, France. (e-mail: Jean-Claude.Buriez@univ-lille1.fr; Yves.Fouquart@univ-lille1.fr; Frederic.Parol@univ-lille1.fr.)

J. Descloitres, NASA Goddard Space Flight Center, Code 922, Greenbelt, MD 20771. (e-mail: jack@ltpmail.gsfc.nasa.gov)

(Received March 31, 1997; revised February 12, 1998;
accepted February 17, 1998.)